

Ultrashort Light Pulses

A. J. DeMaria, D. A. Stetser, W. H. Glenn, Jr.

At the second Quantum Electronics Conference, in 1961, Hellwarth (1) pointed out that if one constructs a pulsed ruby laser with external reflectors and inserts a closed shutter in the optical feedback path, the device will not oscillate and a large overpopulation of the upper laser level will result. If the shutter is opened when the overpopulation is at a maximum, the radiation within the feedback interferometer builds up rapidly and an extremely large output burst of radiation is generated. The desired shuttering action was first achieved with a Kerr cell by McClung and Hellwarth (2), with a rotating disk by Collins and Kisliuk (3), and with an ultrasonic-refraction shutter by DeMaria, Gagosz, and Barnard (4). Rotating mirrors and prisms, Pockel cells, and saturable absorbers (5-7) have also been used. The minimum pulse widths obtainable with these various experimental techniques are limited to approximately 10^{-8} second because of the requirement of one or more passes through the laser medium to build up the laser pulse. Peak powers of approximately 5×10^8 watts have been obtained with these techniques. Hellwarth's method of generating short laser pulses of high peak power is often referred to as "laser Q -switching" because Q is a resonator's figure of merit, defined as the ratio of the energy stored to the energy dissipated within the interferometer in a time interval $1/2\pi$ times the period of the optical oscillations. The

availability of these Q -switched optical pulses made possible the experimental investigation of such phenomena as optically generated plasmas; optical harmonic generation; stimulated Raman, Brillouin, and Rayleigh-wing scattering; photon echoes; optical electrostriction and Kerr effects; optical parametric amplifications; and high-speed holography.

This article is concerned with recent efforts by our associates and ourselves to generate optical pulses of extremely high peak power (approximately 10^{10} watts) and extremely short duration (of the order of 10^{-13} second). There are numerous reasons why researchers have become interested in the generation of such optical pulses. Numerous applications, in the aforementioned areas of research, of single and multiple high-peak-power laser pulses of 10^{-9} - to 10^{-13} -second duration are potentially very attractive. An optical pulse of 10^{-13} -second duration at a wavelength of approximately 1 micron rises from zero to 10^{10} watts in approximately 50 optical cycles; 10^{-13} second is the time required for light to travel 0.003 centimeter, and 10^{-3} centimeter therefore represents the length of this wave packet of light. The interaction of such extremely short, high-power light pulses with both organic and inorganic matter is therefore of great interest to academic, military, and industrial researchers. The application of such pulses to research on optically generated plasmas, optical radar, optical computers, high-speed photography and holography, optical and vibrational spectroscopy of liquids, solids, and gases, nonlinear optical properties of materials, photon echoes, precursor wave studies, transient response

of optical instruments, velocity of light measurements, and so on, appears very promising. For example, such pulses would make it possible to measure distances of many kilometers to within fractions of a millimeter. Since atoms radiate for 10^4 or more optical cycles, such pulses would make possible experimental investigation of the impulse response of quantum systems and of optical instruments. Electrical pulses having a rise time of less than 10^{-10} second, amplitudes of 60 to 100 volts, and repetition period as short as 1.5 nanosecond have already been obtained through use of fast photodiodes as detectors (8). Electrical pulses with these characteristics were previously unattainable. Such electrical pulses should find application in the electronics industry, for determining the location and severity of internal reflections in wide-bandwidth transmission systems, studying propagation delay, making bandwidth measurements, and so on.

Method for Generating Ultrashort Laser Pulses

It is well known, from the Fourier theorem, that any repetitive pulse train having a time-dependent amplitude $E(t)$ and a fixed period τ can be represented by a series of discrete sinusoidal functions having integrally related frequencies and fixed phase relationships:

$$E(t) = \frac{E_0}{2} + \sum_{m=1}^{\infty} \left[E_m \cos\left(\frac{2\pi mt}{\tau}\right) + E_m' \sin\left(\frac{2\pi mt}{\tau}\right) \right]. \quad (1)$$

The frequencies are all multiples of $1/\tau$, and the narrower the pulse width $\Delta\tau$ (defined as the full width at half-amplitude), the larger the bandwidth required to reproduce the repetitive pulse train.

A laser oscillator essentially consists of an active medium, having a complex refractive index as given by $n = n_0 - ik$, which is inserted between two reflectors separated by a distance L . The pa-

Dr. DeMaria is principal scientist, quantum physics; Mr. Stetser is research scientist, quantum physics; and Dr. Glenn is senior research scientist, quantum physics, Research Laboratories, United Aircraft Corporation, East Hartford, Connecticut.

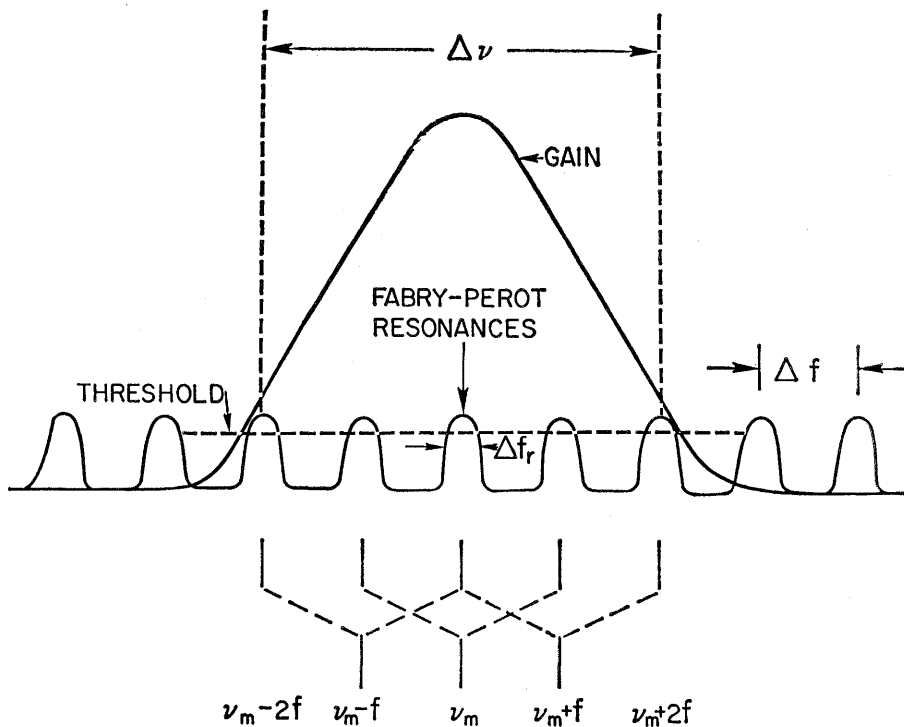


Fig. 1. Visual representation of the gain of the laser line profile with the resonances of the Fabry-Perot interferometer superimposed.

parameter $\omega k/c$ is the gain per unit length (or Lorentz's index of absorption, if the sign of the complex-refractive-index portion is positive) where ω is the optical angular frequency and c is the velocity of light in free space. The resonances of such a system are determined by the spectral line width of the laser transition and by the number of half-wavelengths existing between the two reflectors. The gain of a laser line profile superimposed on the resonances of a Fabry-Perot interferometer is illustrated in Fig. 1. The interferometer resonant frequency ν_m is given by $\nu_m = mc/2Ln_0$. These resonances are the axial mode resonances of the interferometer. The frequency separation Δf between two adjacent axial resonances is given by $\Delta f = c/(2Ln_0)$. The round-trip transit time (τ) for a pulse of light to bounce back and forth between the two mirrors is given by $\tau = 2Ln_0/c = 1/\Delta f$.

It is now evident that means are available within a laser oscillator for the generation of a periodic pulse train of coherent light by use of the Fourier series principle. The only requirement that is not met is a means of phase-locking the discrete oscillating frequencies of the laser (that is, providing a fixed phase relationship between the many discrete frequencies). This phase-locking element may be added as follows. It is reasonable to assume that one

resonance ν_m will be nearest the peak of the laser gain profile and will therefore be the first to oscillate. If an amplitude modulator operating at a frequency f is inserted into the laser's feedback interferometer, the frequency ν_m will be amplitude-modulated at a frequency f such that its time-dependent electric field amplitude $E(t)$ will be of the form

$$E(t) = E(1 + M \cos 2\pi ft) \cos 2\pi \nu_m t, \quad (2)$$

where M represents the modulation index (that is, the degree of modulation). By expansion of Eq. 2, the equation of a wave with a simple sinusoidal amplitude modulation can be written in the form

$$E(t) = E \cos 2\pi \nu_m t + \frac{ME}{2} \cos 2\pi(\nu_m - f)t + \frac{ME}{2} \cos 2\pi(\nu_m + f)t. \quad (3)$$

If the modulating frequency f is chosen to be commensurate with the axial mode frequency separation ($f = \Delta f$), superposition of the upper $(\nu_m + f)$ and lower $(\nu_m - f)$ side bands of the amplitude-modulated light beam with the adjacent resonances couples the $(\nu_m + f)$, $(\nu_m - f)$, and ν_m axial modes with a well-defined amplitude and phase (see Fig. 1) (9). As the $(\nu_m + f)$ and $(\nu_m - f)$ oscillations pass through the modulator, they also become amplitude-modulated. Their

side bands, in turn, couple the $(\nu_m + 2f)$ and $(\nu_m - 2f)$ axial modes to the previous three modes. This process continues until all axial modes falling within the oscillating line width are coupled. The constructive and destructive interference of these simultaneous phase-locked oscillations is analogous to the interference of Fourier-series components in the construction of a repetitive pulse train.

Let us assume that at time $t = 0$, m sinusoidal components of amplitude E and circular frequencies $\omega_1, \omega_2, \dots, \omega_m$ all have identical phases such that they are all aligned along the x -axis of the phasor diagram of Fig. 2a. Let us assume also that all the frequencies are integral multiples of some angular frequency ω . The resultant (R) of all the amplitudes is $R = mE$. At some later time t' , the frequency ω_m has rotated an angle $\alpha_m = \omega_m t'$ from the x -axis. The angle θ between any two adjacent modes is given by

$$\theta = \frac{(\omega_m - \omega_1)t'}{n - 1}. \quad (4)$$

At some later time $t = \Delta\tau$, the angle θ equals $2\pi/m$ and $R = 0$, as illustrated by Fig. 2c. Solving Eq. 4 for $t' = \Delta\tau$ gives

$$\Delta\tau = \frac{m - 1}{m \Delta\nu}, \quad (5)$$

where $\Delta\nu = (\omega_m - \omega_1)/(2\pi)$. For large m , $\Delta\tau \approx 1/\Delta\nu = \lambda_m^2/c\Delta\lambda$, where $\lambda_m = c/\nu_m$ and $\Delta\lambda = \Delta\nu\lambda_m^2/c$. At a still later time $t = \tau$, the components again have identical phases and the angle θ equals 2π and $R = mE$. Solving Eq. 4 for $t' = \tau$ gives

$$\tau = (m - 1)/\Delta\nu. \quad (6)$$

For large m , $\tau \approx m/\Delta\nu$.

The period of the repetitive pulse train is given by Eq. 6, and since $\Delta f = \Delta\nu/m$, $\tau = 1/\Delta f$, as discussed above. The maximum number (m) of active axial modes that can exist within a gain bandwidth $\Delta\nu$ is given by $m = 2L\Delta\lambda/\lambda_m^2$. Since the resultant power of m phase-locked components is equal to the square of the sum of the components, the peak power of the pulses is m times the average power. Lasers operated in this manner are called "mode-locked" or "phase-locked" lasers.

In the first experimental demonstration of "mode-locking," helium-neon and argon lasers were used (10, 11). The relatively narrow spectral line widths of gas lasers limit pulse widths to the order of 10^{-10} second (that is, $\Delta\nu \approx 10^{10}$ hertz). On the other hand,

the broader line widths available in solid-state lasers can be expected to produce considerably narrower pulses. The results of mode-locking experiments with solid-state lasers such as glass doped with neodymium (12, 13), ruby (14), or yttrium aluminum garnet-neodymium (YAlG-neodymium) (15) have been reported. A direct pulse-width measurement of 1.5×10^{-10} second and an indirect measurement yielding a lower limit of approximately 8×10^{-11} second have been reported for YAlG-neodymium lasers (15).

The glass-neodymium laser is of particular interest for the generation of ultrashort pulses, as a result of its broad oscillating line width of 100 to 200 angstroms at a center wavelength of 1.06 microns (12, 13, 16). With a mirror spacing of $L = 1.5$ meters, there exist approximately 6×10^4 axial interferometer resonances across the 200-angstrom line width, and a pulse width, at the half-intensity points, of 2×10^{-13} second could theoretically be obtained.

Active time-varying-loss (10-12, 14) and reactance (17) modulators have been utilized for mode-locking laser oscillators. Ultrasonic standing wave diffraction cells (18, 19) and KDP Pockel cells (14) have been utilized, among others, as active loss modulators, whereas only Pockel cells have been utilized as reactance modulators (17, 20).

Hargrove, Fork, and Pollack (10) were the first to operate a laser in the mode-locked condition. They employed a helium-neon laser operating at 6328 angstroms and an ultrasonic diffraction modulator (18). When locking of the axial modes had been achieved, Hargrove and his co-workers reported, there was virtual elimination of both random and systematic amplitude fluctuation, as well as a fivefold increase in amplitude. At modulating frequencies far from the adjacent axial-mode beat frequencies, a sinusoidal output was obtained. As the modulating frequency approached the axial-mode frequency separation, the modulated output changed from a sinusoidal to a pulse or "spike" form, with a reduction in pulse width and an increase in peak power. If the modulating frequency f is nearly equal to Δf and is such that f falls within the bandwidth Δf_r of the interferometer resonance [that is, $|\Delta f - f| < (\Delta f_r/2)$], then low-frequency optical beats between the oscillating axial modes and the internally generated side bands can be detected (21).

Mode-locking a laser oscillator with an active modulator requires the critical adjustment of mirror spacing and modulating frequency. Mode-locking a laser by means of the nonlinear gain characteristics of the inverted population (11) requires critical adjustment of (i) the Q of the interferometer, (ii) laser position, and (iii) gain of the system. In addition, both methods require that the laser be compensated for any perturbations in optical length of the feedback interferometer. Such compensation is of particular importance in the mode-locking of large solid-state lasers as a consequence of the variation in optical length of the rods during the optical-pumping flash.

A method has been recently found for automatically obtaining mode-locked laser operation without having to make these critical adjustments. In this method a passive modulator which simultaneously serves as a Q -switch and as an amplitude modulator is utilized (13, 16, 22). It has been recently shown that an optical saturable absorber which has a relaxation time faster than τ is well suited for the role of passive modulator

in mode-locking lasers. An optical saturable absorber operates as a passive modulator in the following way. Let us assume that a pulse of light is incident on a two-level quantum system whose separation energy is equal to the photon energy of the incident light pulse (Fig. 3a). As the pulse propagates through the material, the leading edge of the pulse is heavily absorbed and atoms make transitions from the lower to the upper state (Fig. 3b) of the two-level quantum system. As a result of this process, the absorber tends to saturate (that is, tends to provide less attenuation for the higher-amplitude portions of the pulse and higher attenuation for the lower-amplitude portions). This process represents the opening of the passive modulator. After the pulse has propagated through the system, the atoms make transitions to the lower state; this represents the closing of the modulator (Fig. 3c). Some time later, all the atoms are in the lower state and the modulator is again closed (Fig. 3d). If the pulse is reflected back and forth between two mirrors between which the dye cell and a laser medium have been

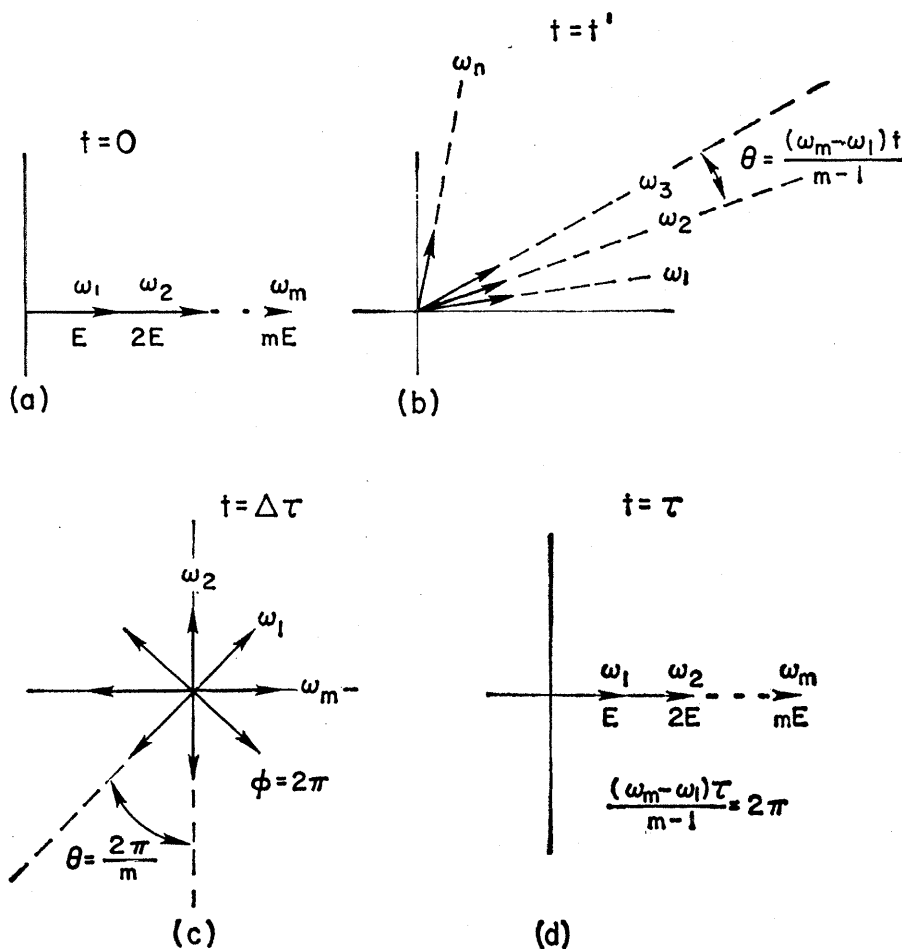


Fig. 2. Phasor diagrams of m phase-locked laser axial modes.

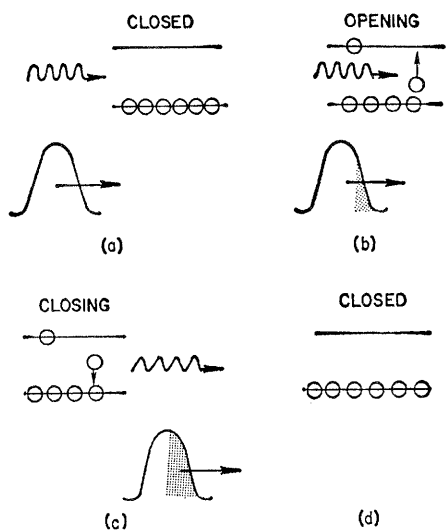


Fig. 3. Basic operations of a saturable-absorber passive modulator.

inserted, the sharpness of the pulse continues to increase until the harmonic content of the pulse equals the overall bandwidth of the system. When this occurs, the pulse cannot become narrower. The action of such a saturable absorber placed within a laser may also be viewed as the action of a shutter or modulator which automatically adjusts its modulating frequency to the round-trip transit time (τ) of the pulse bouncing back and forth between the laser's mirrors. The effect of the passive modulator can be interpreted as a pulse-shaped varying loss having a fundamental frequency equal to the adjacent axial-mode separation frequency Δf . Such a modulating action requires that the relaxation time of the absorber be shorter than τ . The absorption of the leading edge of the

pulse provides a modulator which is rich in multiple harmonics of Δf and results in the phase-locking of many axial modes of the laser.

The passive-modulator mode-locked laser is the optical analog of the electronic regenerative pulse generator described by Cutler (23). This microwave pulse generator consisted of a feedback loop encompassing an amplifier, a filter, a delay line, and a circuit, called the expander (Fig. 4a). The functions of these elements are all well known, with the possible exception of that of the expander; its function was that of providing less attenuation for a high-level signal than for a low-level signal. The expander prevented the degradation (by noise and distortion) of a pulse recirculating indefinitely around the feedback loop, by (i) emphasizing the highest amplitude of the recirculating pulse; (ii) reducing the lower amplitudes; (iii) discriminating against noise and reflections; and (iv) acting to shorten the pulse until the pulse width was limited by the frequency response of the circuit. The output of the electronic regenerative pulse oscillator had a pulse rate equal to the reciprocal of the loop delay, pulse widths inversely equal to the overall system bandwidth, and a center frequency determined by the median filter frequency.

A laser possesses all the basic elements of Cutler's regenerative pulse generator, with the possible exception of the expander element (Fig. 4b). The laser medium serves as the amplifier, the combination of the Fabry-Perot resonances and the line width of the laser transition serves as the filter, and the

time required for an optical pulse to traverse twice the distance between the reflectors serves as the loop time delay. The optical analog of the electronic expander is the saturable absorber, such as the reversible-bleachable dye solutions commonly used as laser Q -switches. The requirements for the saturable absorber are (i) that it have an absorption line at the laser wavelength, (ii) that it have a line width equal to, or broader than, the laser line width, and (iii) that the dye's recovery time be shorter than the loop-time-delay of the laser.

As mentioned earlier, the glass-neodymium laser is of particular interest for the generation of ultrashort pulses, as a result of its broad line width. The availability of saturable absorbers (for example, Eastman-9740 reversible dye solution) for use as an optical expander element at 1.06 microns increases the advantages of the glass-neodymium system for the generation of high-peak-power laser pulses of less than 1-nano-second duration.

Ultrashort-Laser-Pulse Experiments

Experiments on simultaneous Q -switching and mode-locking, with saturable dyes, were performed with an Nd^{3+} -doped glass rod 12.2 centimeters long and 0.95 centimeter in diameter. The ends of the rod were polished at the Brewster angle to eliminate back reflection at the end surface. Two external dielectric reflectors having reflectivities of 99 and 70 percent, respectively, were utilized for the laser's feedback interferometer. The reflectivities of the feedback interferometer were found not to be critical for obtaining mode-locking. The rod was optically pumped with linear flash lamps which were optically coupled to the rod with closely wrapped silver foil. The response time of the overall detection system [an ITT model-F4018 (S-1) biplanar photodiode and a Tektronix model-519 traveling wave oscilloscope] was just under 0.5×10^{-9} second. Eastman-9740 reversible dye solution was used as the saturable absorber. The optical cell containing the dye was placed within the feedback interferometer near one or the other of the two reflectors. Position of the rods as a function of distance from either reflector was found not to be critical.

Through judicious adjustment of the absorption coefficient of the dye solution and adjustment of the voltage of the flash lamp's capacitor bank, we were able to record the tendency of the satu-

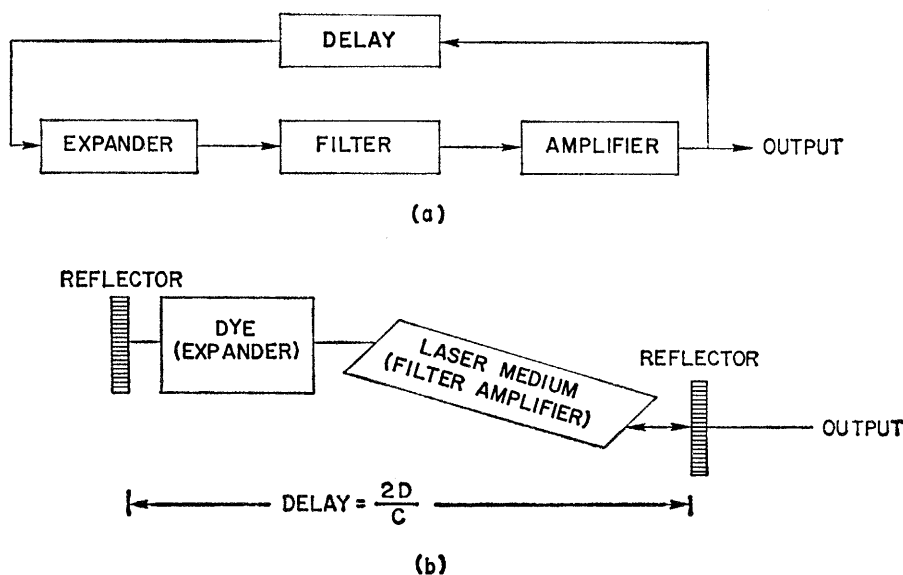


Fig. 4. Equivalence of (a) Cutler's regenerative pulse generator and (b) a laser with a saturable absorber inserted within its feedback interferometer.

rable dye to emphasize the highest amplitude fluctuation occurring at the initiation of laser oscillation and to shorten this fluctuation's pulse width as it successively propagates through the saturable absorption cell, as illustrated in Fig. 5 (top). Figure 5 (top) is an oscillogram of the laser's output for 3×10^{-8} second (sweep speed, 5×10^{-9} second per division) of the early portions of a slow-buildup, Q -switched pulse. The initial periodic amplitude fluctuations are caused by the beating of two axial modes separated by a frequency of $2\Delta f$. At the end of 3×10^{-8} second, the smaller peak of the amplitude fluctuation is almost completely eliminated, the pulse half-width is reduced to 0.5×10^{-9} second, and the pulse-repetition period ($\tau = 2.5 \times 10^{-9}$ second) is equal to $2L/c$, where L is the optical path length (37.5 centimeters in this case) between the reflectors. An oscillogram of an entire simultaneously mode-locked and Q -switched pulse, at a sweep speed of 2×10^{-7} second per division, is illustrated in Fig. 5 (middle). As the pumping intensity was increased, multiple Q -switched pulses occurred. Figure 5 (bottom) depicts the mode-locked output of the laser at a sweep speed of 10×10^{-9} second per division. The recorded pulse half-widths are approximately 5×10^{-10} second, and the repetition period is 9.2×10^{-9} second for an optical round-trip path length of 276 centimeters between the reflectors. Notice that the rise time of the pulse equals the overall rise time of the system ($\sim 5 \times 10^{-10}$ second per division). The fall time is larger than the rise time as a result of critical damping of a resonance at approximately 850 megahertz within the ITT model-F4018 (S-1) biplanar photodiode. The best instrument-limited electronic measurement of the pulse width obtained to date is 1.5×10^{-10} second. For this measurement a modified traveling-wave oscilloscope (Tektronix model-519), having a frequency response from zero hertz to 3 gigahertz, was used, together with a type-T5192 coaxial deflection cathode ray tube and an ITT model-F4014 diode. If the rise time (1.3×10^{-10} second) of the modified oscilloscope is subtracted from the measurement, a pulse width of less than 9×10^{-11} second is obtained. With such combinations of mode-locked laser and fast detector, electrical pulses having amplitude of 100 volts, pulse widths of slightly less than 9×10^{-11} second, and repetition rates of 2×10^{-9} second have been obtained. Electrical pulses with these characteristics were previously un-

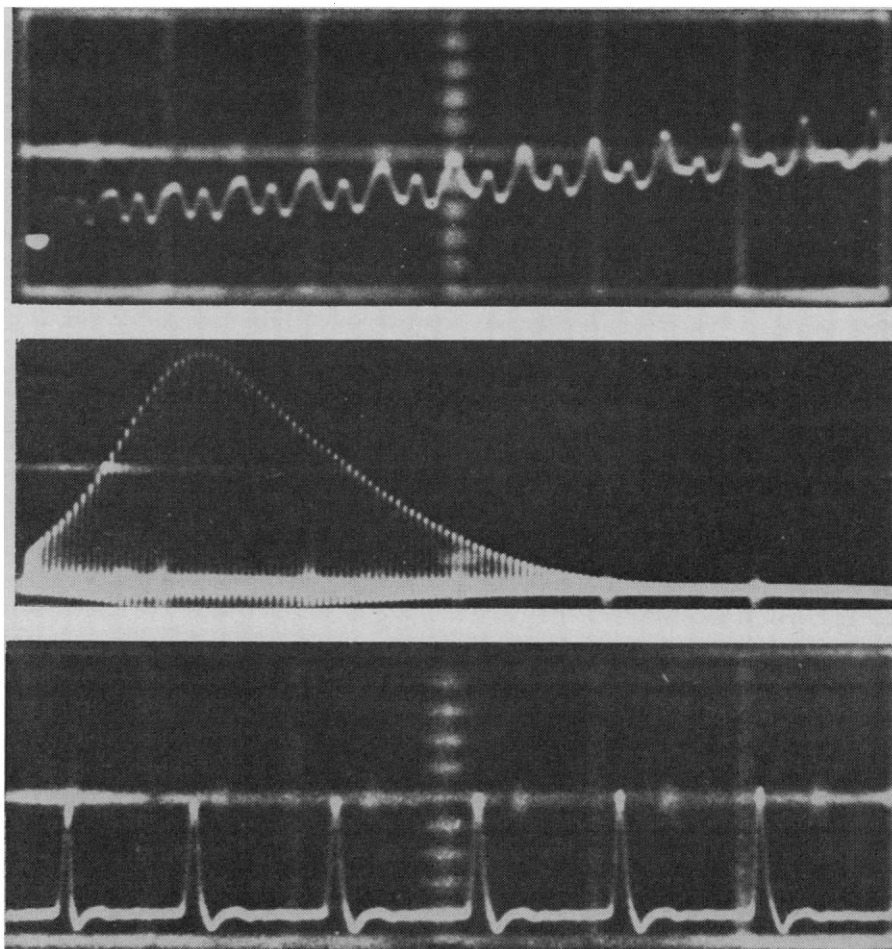


Fig. 5. Oscillograms of the output of a simultaneously Q -switched and mode-locked Nd^{3+} -doped glass laser. Sweep speed, (top) 5×10^{-9} second per division; (middle) 2×10^{-7} second per division; (bottom) 10^{-8} second per division.

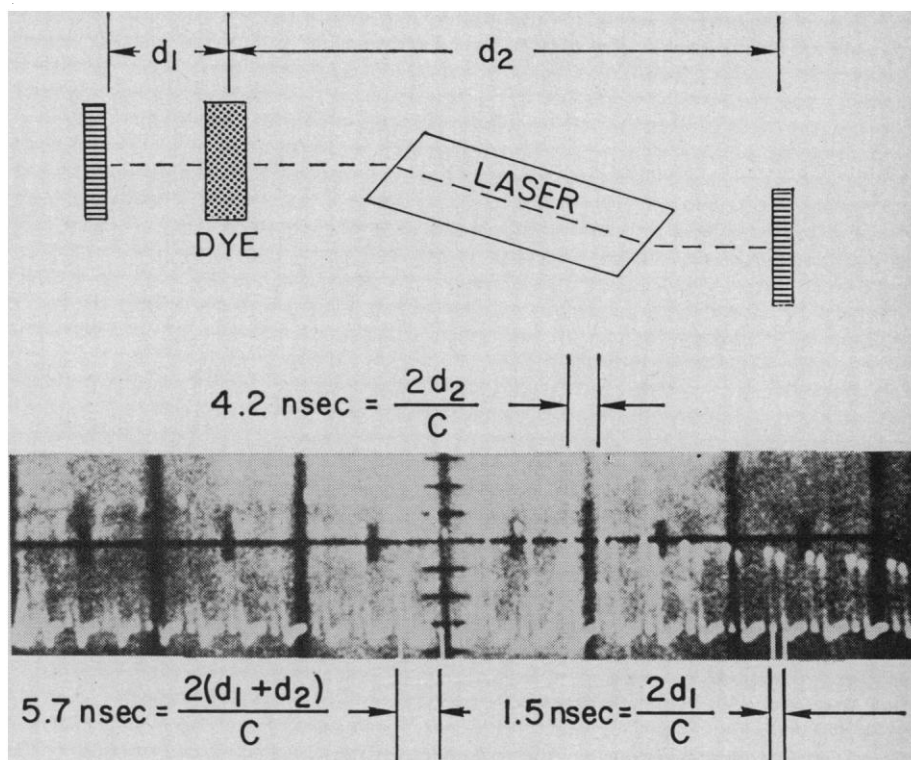


Fig. 6. Double pulsing of a mode-locked laser. (Top) Experimental arrangement; (bottom) oscillogram of the output at a sweep speed of 2×10^{-8} second per division.

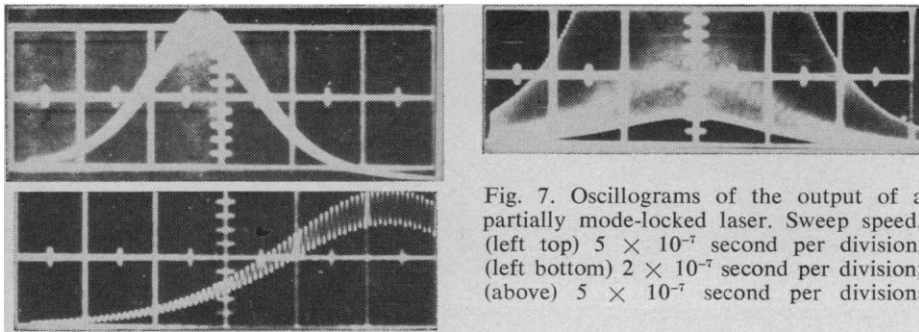


Fig. 7. Oscilloscopes of the output of a partially mode-locked laser. Sweep speed, (left top) 5×10^{-7} second per division; (left bottom) 2×10^{-7} second per division; (above) 5×10^{-7} second per division.

attainable; such pulses should find application in the electronics industry. A calculation based on the 9×10^{-11} -second measurement yields a peak power of approximately 20×10^6 watts.

If the dye cell is moved a distance d_1 from the left-hand mirror of the laser oscillator, as illustrated in Fig. 6 (top), the double pulsing illustrated by Fig. 6 (bottom) results. The pulse spacings are all related to the transit time between the distances d_1, d_2 and $D = d_1 + d_2$. This occurrence may be explained as follows.

Let us assume that, at $t=0$, two pulses exist at $x = d_1$. After $t=0$, the pulses travel in opposite directions, and the time separation between the pulses will vary from zero to a maximum of $t = 2d_1/c$. The pulses will cross every $t = D/c$ second, and the pulse-cross-over points will alternate between the points $x = d_1$ and $x = D - d_1$. The pulses will therefore simultaneously cross through the dye every $t = 2D/c$ second. If two pulses are going to bounce back and forth between the two

reflectors of the laser, this time relationship between the pulses corresponds to the condition of minimum loss. If the dye cell is placed in the center of the laser cavity ($d_1 = d_2$), then the pulse period changes from $\tau = 2L/c$ to $\tau = L/c$. It has been noted in this case that occasionally one of the pulses is wider than the other; this indicates that the two pulses propagating in opposite directions are independent of one another. Figure 7 shows oscilloscopes of the output of a partially mode-locked laser. Since not all of the oscillating modes are phase-locked, the destructive interference is not complete and gives rise to an amplitude fluctuation riding on a continuous level (Fig. 7, left top and bottom). As a larger percentage of the oscillating axial-modes are phase-locked, the ratio of the amplitude fluctuation to the continuous output level decreases (see Fig. 7, right), until finally, when all the oscillating modes are phase-locked, the output illustrated by Fig. 5, middle and bottom, is obtained.

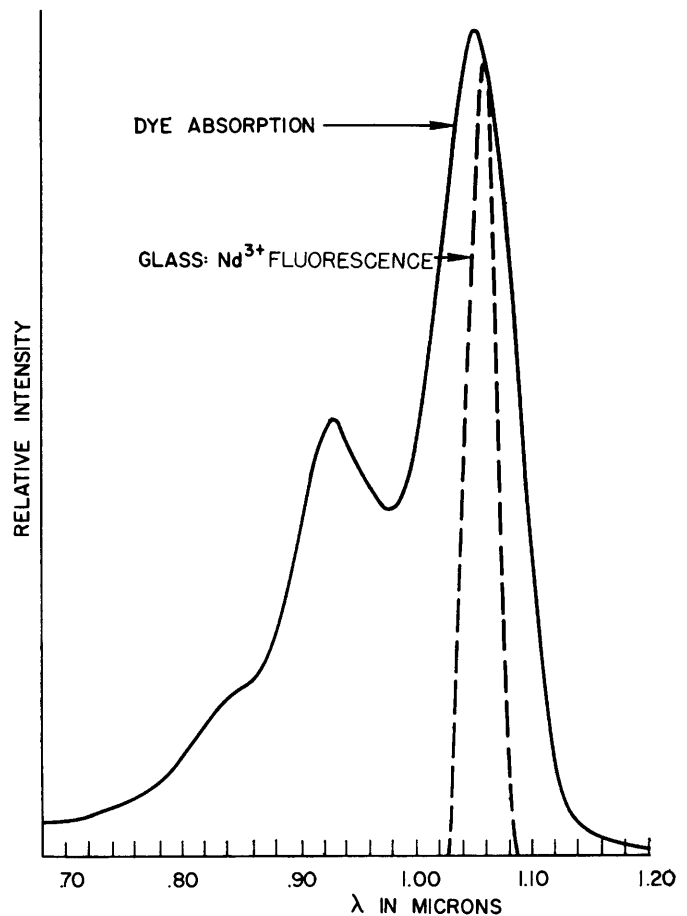
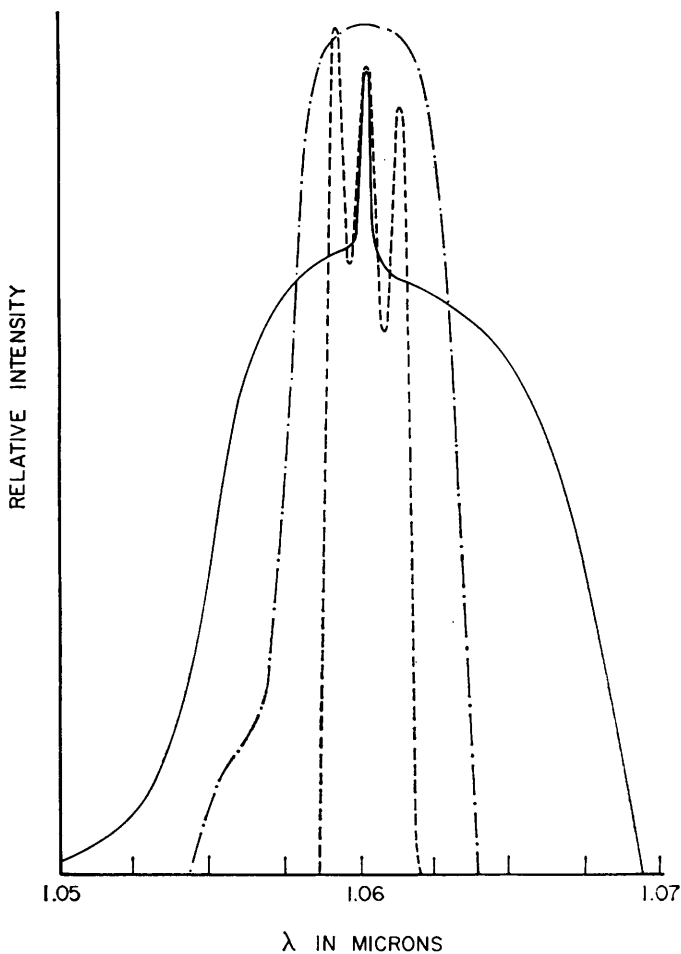


Fig. 8 (left). Comparison of the spectral characteristics of the output of (dashed line) a normal Kerr-cell-operated neodymium-doped glass laser; (dashed-and-dotted line) a Q -switched neodymium-doped glass laser; and (solid line) a simultaneously Q -switched and mode-locked neodymium-doped glass laser. Fig. 9 (right). Superposition of the low-intensity absorption line of an Eastman-9740 saturable absorber dissolved in chlorobenzene and the laser line profile obtained with a neodymium-doped glass laser.

**Measurements of
Ultrashort Laser Pulses**

Direct measurements of the duration of optical pulses are most often made by displaying, by means of an oscilloscope, the output of a suitable photodetector illuminated by the optical radiation. A high-speed germanium photodiode and a sampling oscilloscope have been utilized in this manner to obtain a direct pulse-width measurement of 1.5×10^{-10} second for a mode-locked continuous-wave YAlG-neodymium laser (15). A power spectrum measurement made by means of a scanning Fabry-Perot interferometer yielded an indirect measurement of 7.6×10^{-11} second for this experiment. This indirectly measured value was verified by comparing the average second-harmonic power generated in LiNbO_3 driven by the mode-locked laser with the second-harmonic power obtained when the crystal was driven by the normal or unlocked laser. On the basis of an effective coupling of some 40 modes, the peak power of the mode-locked YAlG-neodymium laser used in these experiments was reported to be approximately 4 watts (15).

The ratio of second-harmonic to fundamental power is increased when mode-locked lasers are used, as a consequence of the fact that second-harmonic frequencies produced by the mixing of the different axial-mode fields have fixed phase relationships. The second-harmonic frequencies produced by the mixing of different axial-mode fields of non-mode-locked lasers do not have fixed phase relationships. The enhancement ratio R' , defined as the ratio of the mode-locked second-harmonic power to the normal second-harmonic power, is given by $R' \approx m/3$ for $m > 3$, where m is the number of phase-locked modes (24).

The use of a sampling oscilloscope greatly facilitates the pulse-duration measurement of continuous-wave mode-locked lasers. The relatively short overall duration (approximately 0.50 to 2.50×10^{-7} second) of the repetitive pulse train obtained from a simultaneously Q -switched and mode-locked laser precludes the use of sampling oscilloscopes and necessitates the use of traveling-wave oscilloscopes. Unfortunately, traveling-wave oscilloscopes require large signal inputs and have narrower bandwidths than sampling oscilloscopes (the Tektronix model-519 traveling-wave oscilloscope has sensitivity of ~ 10 volts

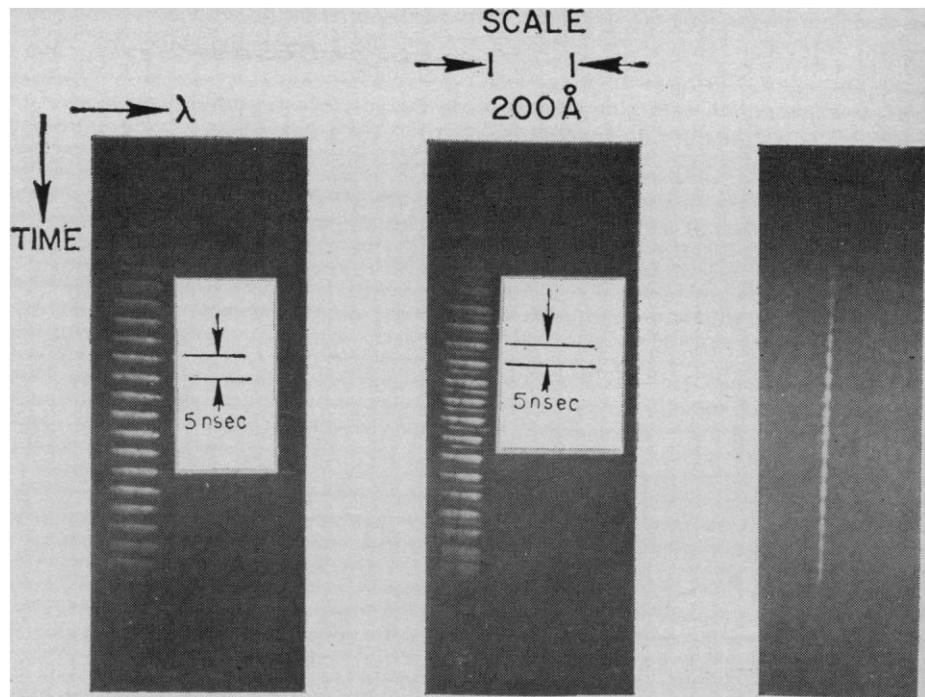


Fig. 10. Time-resolved spectra of (left) properly mode-locked, (middle) double-pulsing, and (right) partially mode-locked output of a neodymium-doped glass laser. Streak duration, 5.0×10^{-8} second per division.

per centimeter and bandwidth of 1 gigahertz). Nevertheless, an instrument-limited direct measurement of 1.5×10^{-10} second has been reported for a simultaneously Q -switched and mode-locked glass-neodymium laser, obtained by utilizing a biplanar photodiode, in conjunction with a modified Tektronix model-519 oscilloscope having a type-T5192 coaxial deflection cathode ray tube, a measured bandwidth of 3 gigahertz, and a sensitivity of 217 volts per centimeter (16). Subtraction of the rise time of the traveling-wave oscilloscope,

1.3×10^{-10} second, yields a photodiode-limited duration of less than 9×10^{-11} second for the optical pulses.

As a result of the normally broad oscillating line width of approximately 30 angstroms for a glass-neodymium laser, the power spectrum measurements of the normally operated laser and of the mode-locked laser can be easily compared by means of standard spectrometers. Figure 8 illustrates the spectral characteristics of the output from a Brewster-ended neodymium-doped glass rod, 12.2 centimeters long and

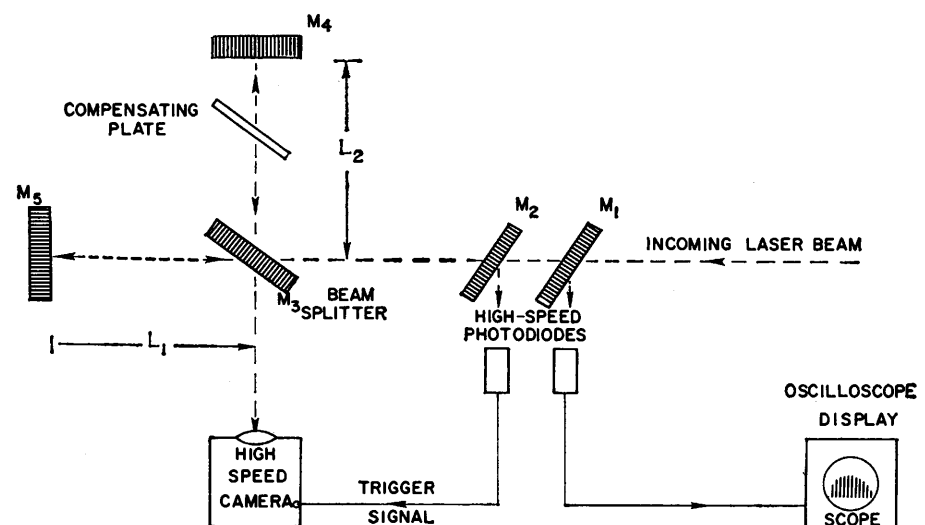


Fig. 11. Experimental arrangement for measuring the correlation function of an ultrashort laser pulse. M , mirror.

0.95 centimeters in diameter, (i) operated normally, (ii) *Q*-switched by means of a Kerr cell, and (iii) simultaneously *Q*-switched and mode-locked. An Eastman-9740 saturable absorber was utilized as the optical expander element. The spectra were obtained with a 3.4-meter Jarrell-Ash spectrometer. The spectra were taken at a constant output energy. The Kerr-cell, *Q*-switch type of operation yielded a uniform spectral width of approximately 50 angstroms. Overexposure of the film by overlapping the spectra of four or more pulses obtained with the Kerr cell, *Q*-switch technique still revealed a power spectrum of approximately 50 angstroms with sharply defined ends. The spectrum of the neodymium-doped glass rod, simultaneously *Q*-switched and mode-locked, with the dye cell placed at the Brewster angle, revealed a uniformly distributed spectrum 180 angstroms wide, with long leading and trailing edges. The increase in spectral width results from the tendency of the saturable-absorber expander element to distribute the energy evenly throughout the spectral line width of the laser medium by the generation of side bands at the resonances of the Fabry-Perot

interferometer. To a first approximation, the minimum pulse widths obtainable with the harmonic content revealed by the spectral data are 2×10^{-13} second, with a corresponding peak power of 10^{10} watts. A calculation of the peak power based on the instrument-limited measurement of 1.5×10^{-10} second yields a peak power of approximately 13×10^6 watts.

Closer observation of the spectrum of the simultaneously *Q*-switched and mode-locked laser of Fig. 8 reveals a relatively intense line at 1.06 microns (the peak of the neodymium gain line). This sharp line is believed to arise from the relatively slow buildup rates of the modes within a passive *Q*-switched laser. For example, in a fast-switched laser oscillator (that is, one switched with a Kerr cell, rotating prism, and so on), the pulse buildup requires approximately ten to 40 loop transits, whereas, for a passive *Q*-switched laser, this buildup requires typically several hundred to a thousand transits (25). Such a long buildup time for the passive *Q*-switched laser supports the view that, for a long time before an appreciable sharpening takes place, relatively few

axial modes exist at line center. It is well known that a narrowing of the output spectrum of fast-switched lasers can be obtained if a saturable absorber having a long relaxation time is placed with the laser feedback interferometer (26). Hercher reported having consistently obtained emission in a single axial mode from a saturable-absorber *Q*-switched ruby laser and a resonant reflector (27). The spectral bandwidth of Hercher's laser was less than 0.001 angstrom (60 megahertz) and was apparently limited by the pulse duration of the *Q*-switched pulse. At this point it is well to mention that passive *Q*-switches can be utilized to either narrow or expand the harmonic content of a *Q*-switched laser oscillator. Saturable absorbers having a relaxation time that is long with respect to the round-trip transit time of an optical pulse bouncing back and forth between the two reflectors tend to narrow the spectrum, while saturable absorbers having a short relaxation time tend to broaden the spectral content of *Q*-switched lasers.

A still closer inspection of the spectrum of the simultaneously *Q*-switched and mode-locked laser of Fig. 8 reveals

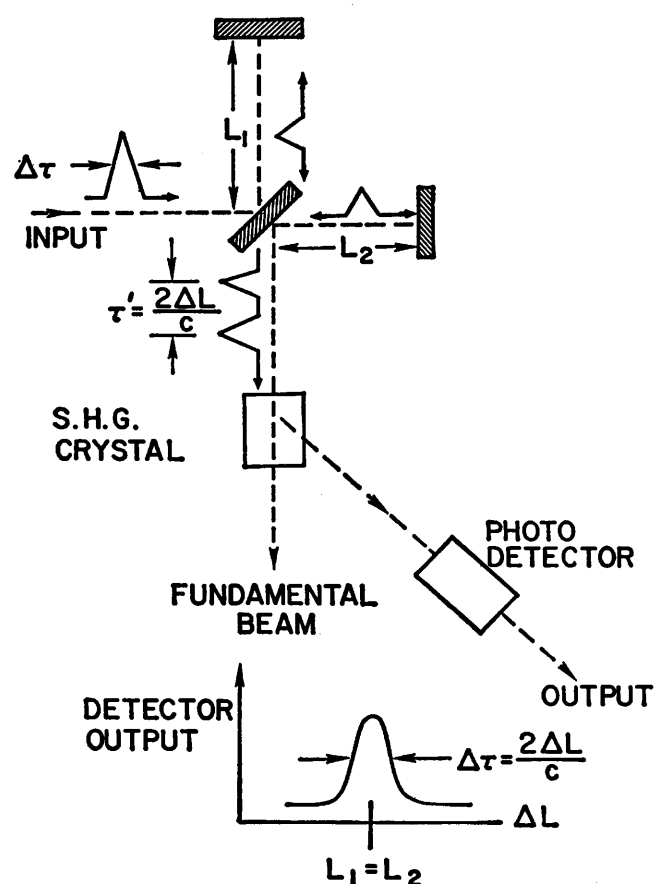
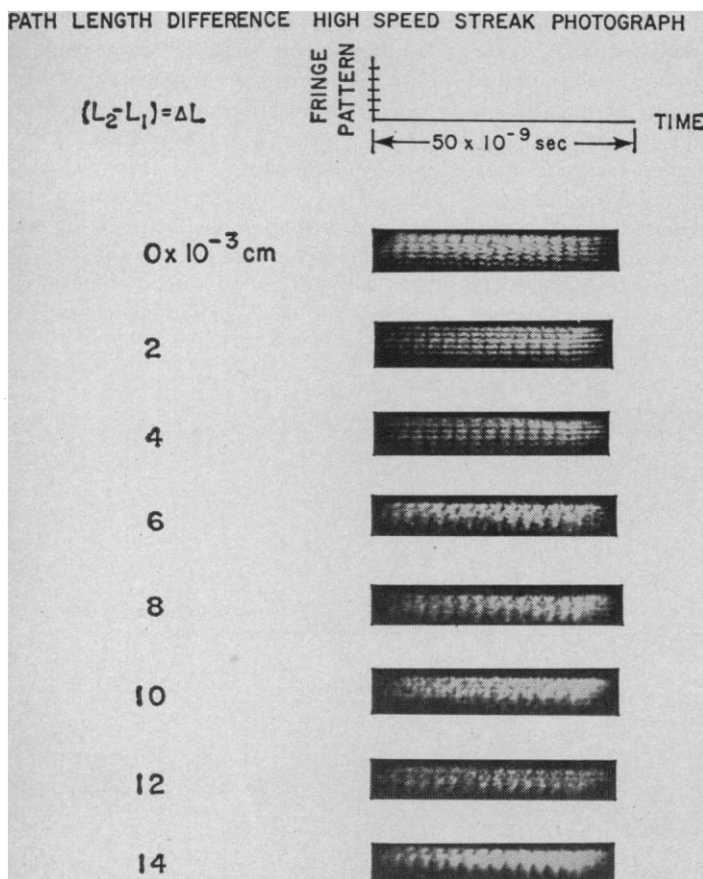


Fig. 12 (left). Variation of the visibility of Michelson's interferometer fringes of ultrashort laser pulses occurring in the middle of the repetitive pulse train, as a function of variation in length of one leg of a Michelson interferometer. Fig. 13 (right). Experimental arrangement for measuring ultrashort optical pulses.

an asymmetrical distribution of the spectral content about line center. The spectrum shows a tendency to expand toward the long-wavelength region under mode-locked conditions. The frequency broadening toward longer wavelengths may be caused by a modulation of the index of refraction at the different frequencies of two or more light components (28), but we believe it more likely that the effect is caused by the fact that the peak of the laser line profile falls on the slope of the long-wavelength side of the absorption line of the Eastman-9740 saturable absorber, as illustrated by Fig. 9. This insures less absorption and, therefore, higher overall system gain toward the longer-wavelength region of the oscillator spectrum.

In order to determine the spectral extent of the mode-locked pulses, a movable diode and slit were placed in the exit focal plane of the spectrometer. Data on the temporal behavior of selected 1- and 0.5-angstrom regions of the spectra were obtained and compared with the simultaneously recorded data of the input pulse train. It was found that the pulse-width measurements of the radiation emitted by the limited spectral region were still instrument-limited. This is to be expected, since the number of modes available in these limited apertures is still sufficient to produce pulses of the order of 3.6×10^{-11} and 1.8×10^{-11} second. Since no change in pulse shape or pulse width was observed in random samplings consisting of 0.6- and 0.3-percent portions of the total input spectral range, it may be concluded that mode coupling is extensive over the entire 180-angstrom spectral output. In addition, time-resolved spectroscopic data obtained with an image-converter streak camera used in conjunction with the 3.4-meter grating spectrometer revealed spectral width of 100 to 120 angstroms for each individual pulse of the repetitive pulse train. Figure 10, left, middle, and right, shows the time-resolved spectra of, respectively, a properly mode-locked, a double-pulsing, and a partially mode-locked glass-neodymium laser output. The streak duration was 5×10^{-8} second, and the pulse repetition period was 5×10^{-9} second. The narrowing of the spectral width for the partially mode-locked pulse is clearly evident.

In the work described above, the power-spectrum density of the periodic pulse train was measured by means of a square-law detector and a grating spec-

trometer. Such a density measurement gave a lower limit of approximately 10^{-13} second for the pulse width. If one pulse is passed through a Michelson interferometer having legs of equal lengths, an interference fringe pattern is recorded on a film placed at the exit. As one leg of the interferometer is increased (or decreased) by a distance ΔL , the recorded fringe pattern will continue to decrease in sharpness until it "washes" out for a length change $\Delta L = (c\Delta\tau/2) = (c/2\Delta\nu)$, where $\Delta\tau$ is the pulse width and $\Delta\nu$ is the spectral width of the

pulse. The interference pattern is thus the correlation function for the pulse. Since the power-spectrum density and its correlation function are a Fourier-transform pair, complete information about the frequency distribution (and, thus, the pulse width) of the average energy of the periodic pulse train is therefore contained in its correlation function. It is therefore expected that the results of the experiment of Fig. 11 will be identical to those of the experiments of Figs. 8 and 10.

Figure 12 illustrates the variation of

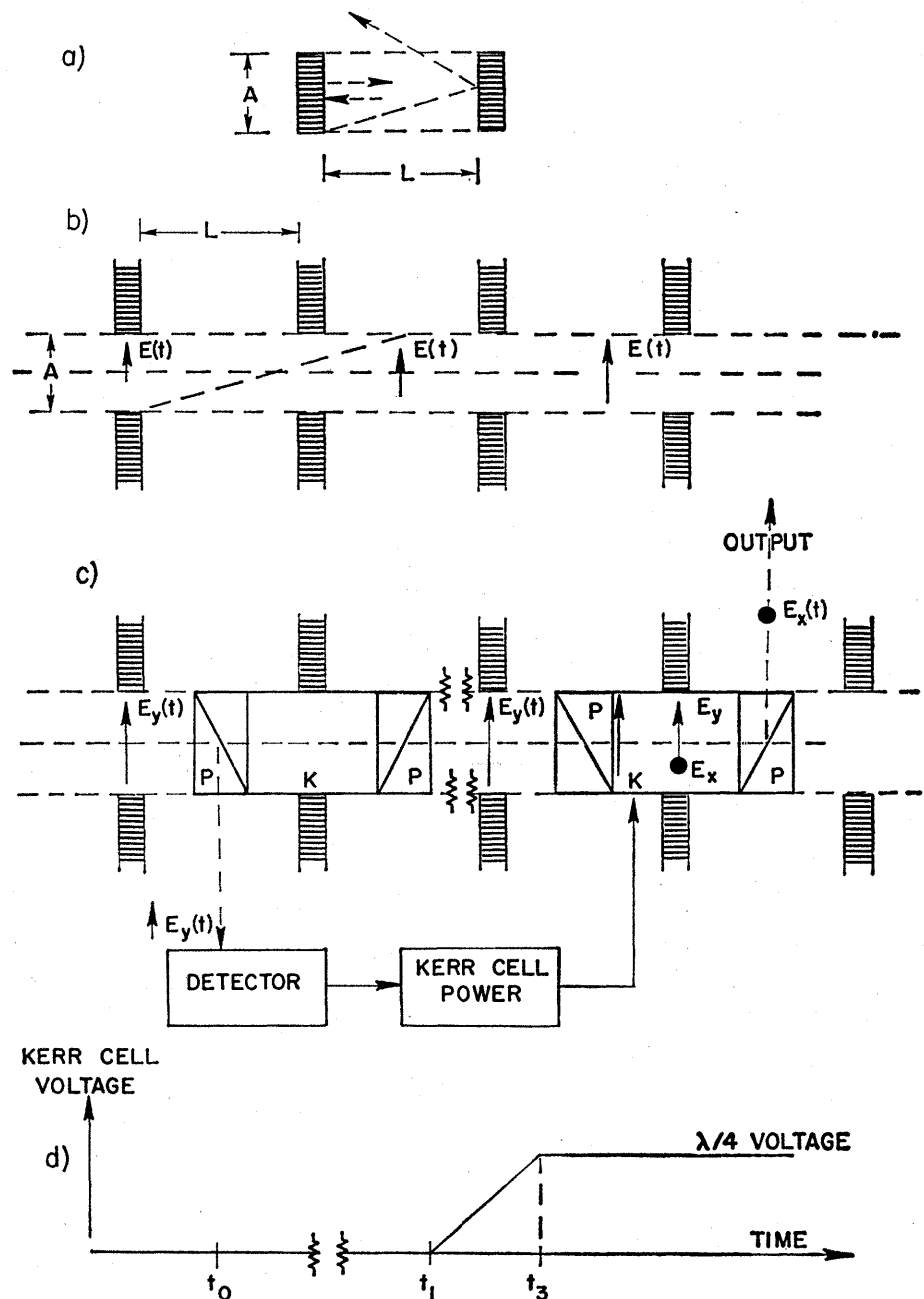


Fig. 14. Basic principles of the mode of operation in which simultaneous *Q*-switching and mode-locking is combined with pulse transmission for obtaining a single ultrashort laser pulse. (a) Typical laser configuration. (b) Transmission line analog. (c) Pulse-transmission mode of laser operation. (d) Time sequence of the switching of the Kerr cell.

the visibility of the fringes of pulses occurring in the middle of the pulse train, as recorded by an image-converter streak camera placed at the exit of the Michelson interferometer, as a function of variation in the length of one leg of the interferometer of Fig. 11. In Fig. 12, time increases from left to right, and the fringe patterns of interest run horizontally. For a ΔL variation from zero to 4×10^{-3} centimeter, the fringe patterns are quite clear; for a ΔL variation from 4×10^{-3} to 8×10^{-3} centimeter, the visibility of the fringe patterns decreases; and for a variation greater than 8×10^{-3} centimeter, the fringes are no longer visible. The minimum pulse width $\Delta\tau$ for a ΔL of 8×10^{-3} is $\Delta\tau = 5 \times 10^{-13}$ second. It was found that, if an integrated record and not a time-resolved record of the fringe pattern was obtained, the minimum pulse width increased by an order of magnitude. This result indicates that the time duration of the pulses varies from pulse to pulse.

A true measurement of the pulse width may be obtained with the experimental arrangement shown schematically in Fig. 13. In this experiment the film at the exit of the interferometer is

replaced with a second-harmonic generator. The incoming pulse to the interferometer is split up into two pulses each having an amplitude E . If $L_1 \neq L_2$, these two pulses are separated in time τ by $\tau = [2(L_1 - L_2)/c] = 2\Delta L/c$. These two pulses of infrared radiation produce a pulse of green radiation leaving the second-harmonic generator crystal, having an amplitude γE^2 , where γ is a constant of the crystal which denotes the efficiency of the conversion from infrared to second-harmonic green radiation. The output from a photodetector utilized for detecting the second-harmonic pulses is given by $2\alpha\gamma^2 E^4$, where α is a constant of the detector. As the legs of the interferometer are adjusted in such a way that $L_1 \rightarrow L_2$, the second-harmonic intensity and the photodetector output increase. When $L_1 = L_2$, the second-harmonic intensity becomes $4\gamma E^2$, and the output of the detector becomes $16\alpha\gamma^2 E^4$. The bottom diagram of Fig. 13 is a generalized plot of experimental data typically expected from such an experiment. The pulse width is given approximately by $\Delta\tau \simeq L/c$. A Michelson interferometer in combination with an oscilloscope would

provide an automatic means of measuring light pulses of less than 1 picosecond duration; the measurement would be obtained from (i) a recording of the periodic change in the optical length of one leg of the interferometer along the horizontal axis and (ii) the output signal from the vertical axis of the oscilloscope. Such an instrument would be the optical analog of the electronic sampling oscilloscope. The curve typically illustrated by the bottom diagram of Fig. 13 represents the correlation of the energy of the pulse. This additional information is obtained from the experiment of Fig. 13 by means of a fourth-power-law detector (28a).

Method for Generating Single Ultrashort Laser Pulses

The first method proposed for obtaining a single high-peak-power laser pulse having a pulse width narrower than those obtainable from standard Q -switched lasers was proposed by Vuylsteke (29). This method involved Q -switching a laser with mirrors of 100-percent reflectivity on both ends of the cavity, and, at the peak of the pulse, the rapid switching of the output mirror from 100-percent to zero reflectivity. In this manner, the optical energy stored within the cavity would be dumped in the time (τ) required for round-trip transit of the cavity. This type of laser operation, called the pulse transmission mode, was recently reported with calcium tungstate-neodymium and glass-neodymium lasers (30); pulse widths of 4×10^{-9} second, with peak power of 10^7 watts, were obtained. The narrowing of a Q -switched laser pulse of 0.5-joule energy and 1.1×10^{-8} -second duration by passage of the pulse through two saturable ruby amplifiers has also been reported (31). Pulses of 2×10^{-9} -second duration and 15-joule energy for a peak power of 7 to 8×10^9 watts were obtained in these experiments. This second method is general and can be utilized to amplify and reduce the pulse width of any initial pulse.

The experimental technique of Penney and Heynau (32) in combining the simultaneous Q -switching and mode-locking of a neodymium-glass laser by use of a bleachable absorber with the pulse transmission mode is, we believe, of all the experimental methods reported to date, the one capable of yielding the highest peak power with the briefest optical pulses (32, 33). In order to achieve a high probability (p) of suc-

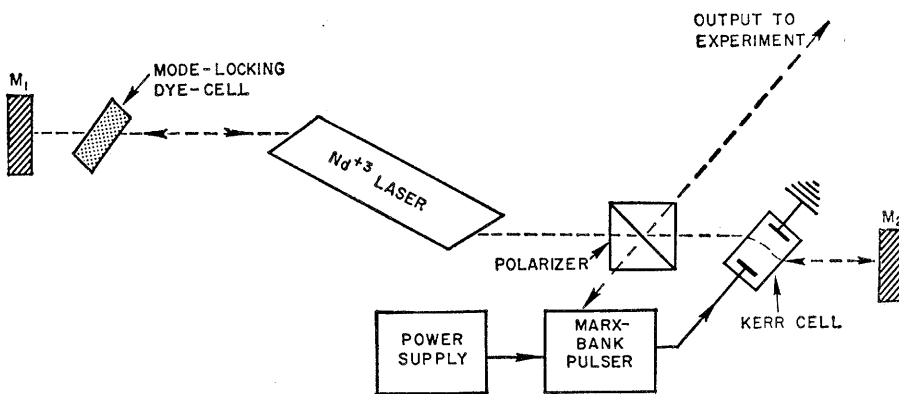


Fig. 15. Typical experimental arrangement for the generation of hundreds of megawatts by laser pulses of less than nanosecond duration. M , mirror.

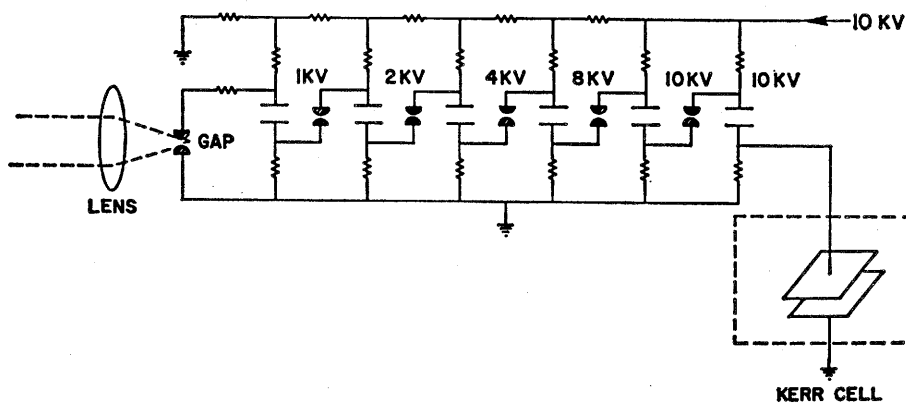


Fig. 16. Schematic diagram of a typical Marx-Bank, Kerr-cell pulser used in the experiment of Fig. 15.

cess ($p > .7$) in selecting a single output pulse with fairly standard electronics for rapid switching of the Kerr cell, they were forced to utilize a laser-feedback-cavity length of approximately 2.5 meters. In the following paragraphs we present in detail a modification of the experimental arrangement of Penney and Heynau which has resulted in the generation of single laser pulses having peak power of hundreds of megawatts (without amplification) and duration of less than a nanosecond, in short optical-feedback cavities (less than 70 centimeters long) (34).

The typical laser configuration of Fig. 14 may be considered to be composed of an infinite series of collinear identical apertures cut into parallel and equally spaced, perfectly absorbing partitions of finite extent, as first suggested by Fox and Li (35). Figure 14b illustrates such a transmission-line analog of Fig. 14a. Light rays propagating at right angles to the apertures propagate through the structure, while off-axis rays are lost to the system as a result of "walk-off" effects. A pulse propagating through the transmission-line structure of Fig. 14b will grow exponentially in amplitude until the gain equals the loss of the system, steady-state operation being thereby achieved. Figure 14c is a diagram of the transmission-line analog of the laser of Fig. 14a with a Glan prism (P) and a Kerr cell (K) inserted near one reflector inside the feedback cavity. When the leakage radiation from the Glan prism incident on a photodetector exceeds a predetermined value, the detector energizes the Kerr cell to its quarter-wave voltage. Let us assume as an example that the optical pulse is initially polarized in the vertical direction. As the pulse propagates through the energized Kerr cell, the polarization develops a horizontal component directed out of the plane of the diagram. For a round-trip traversal of the Kerr cell, the polarization of the pulse is rotated 90 degrees. The forward propagation of a pulse with this polarization is prevented in this system, and the propagation direction of the pulse is redirected by the Glan prism, as illustrated in Fig. 14c. In effect, the high reflectivity of the cavity is suddenly changed to a low reflectivity and the energy initially stored within the cavity is suddenly "dumped." The "dumping" time is limited just by the pulse duration ($\Delta\tau$) if $\Delta\tau < \tau$ (32). If $\Delta\tau > \tau$, the "dumping" time is limited by twice the cavity length, if the Kerr-cell switching time ($\Delta\tau_s$) is $\Delta\tau_s \leq \tau$ (30).

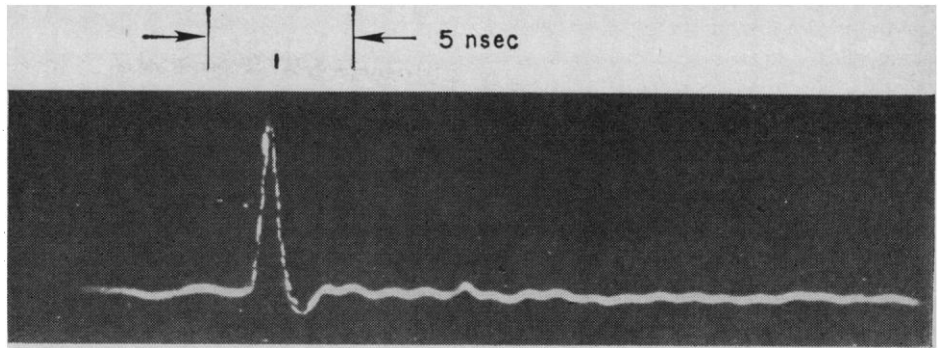


Fig. 17. Oscilloscope trace of a 4×10^{-10} -second single laser pulse of 6×10^8 -watt peak power, generated with the experimental arrangement of Fig. 15.

The experimental arrangement utilized is illustrated in Fig. 15. A Brewster-ended neodymium-doped glass rod 53 centimeters long and 1.3 centimeters in diameter was used, with two mirrors (reflectivity > 99 percent) separated by approximately 70 centimeters. A dye cell, a Glan prism polarizer, and a Kerr cell were placed within the optical cavity. The operation for the overall system was as follows. The Kerr cell was initially energized, and the polarizer was adjusted for maximum transmission. It has been shown that zero initial voltage is best for obtaining a uniform rejection ratio across a Kerr-cell aperture (36). The leakage radiation from the polarizer was focused onto the first gap of a Marx-Bank pulse generator. At the optical pulse amplitude determined by the gap separation, the spark gap broke down, thereby causing rapid successive breakdown of the remaining overvolted spark gaps. Each gap breakdown effectively placed one of a series of six capacitors, charged in parallel, in series with the remaining capacitors. It has been shown that such Marx-Bank pulse generators have a delay of only about 20 nanoseconds from the time of initial gap breakdown to the time of appearance of the high voltage across a load, with jitter time of approximately 1 nanosecond (37). Figure 16 is a schematic diagram of a Marx-Bank, Kerr-cell pulser typical of those used in these experiments. The quarter-wave voltage for the Kerr cell used was 35 kilovolts.

Figure 17 shows a typical oscilloscope trace of a single pulse obtained with the experimental arrangements of Figs. 15 and 16. The recorded full width at the half-intensity points was found, from measurement, to be 0.63 nanosecond; the corresponding energy content was $\frac{1}{4}$ joule. If the response time (0.5 nanosecond) of detector plus oscilloscope is removed from the measurement of

Fig. 17, a pulse width of just under 0.4 nanosecond is obtained, with a corresponding peak power of approximately 6×10^8 watts. The departure of the pulse width from the theoretical limit of 10^{-13} second is believed to be caused by the time variation of the refractive index of the long laser rod and the insertion of the many optical elements into the laser cavity. The fabrication of glass laser rods in lengths of 1 meter or longer offers the possibility of amplifying these pulses up to the limit beyond which the optical flux density would cause destruction of the laser components (34). It has been noted that, when the light-pulse duration is shorter than 10^{-9} second, one can expect an increase in the energy threshold of self-damage, owing to the finite time required for development of the acoustic waves generated by the electrostriction and Brillouin scattering effects (31).

Summary

Experimental techniques are now available for the generation of repetitive and single coherent optical pulses of extremely short time duration and high peak power. These pulses should find extensive application in basic and applied research. Additional shortening of optical pulse durations can be obtained by means of the stimulated Raman effect, second-harmonic generation, or amplification with nonlinear laser amplifiers.

References and Notes

1. R. W. Hellwarth, in *Advances in Quantum Electronics*, J. R. Singer, Ed. (Columbia Univ. Press, New York, 1961).
2. F. J. McClung and R. W. Hellwarth, *J. Appl. Phys.* **33**, 828 (1962).
3. R. J. Collins and P. Kisliuk, *ibid.*, p. 2009.
4. A. J. DeMaria, R. Gagosz, G. Barnard, *ibid.* **34**, 453 (1963).
5. P. P. Sorokin, J. J. Luzzi, J. R. Lankard, G. D. Pettiti, *IBM J. Res. Develop.* **8**, 182 (1964).

6. P. Kofalas, J. Masters, E. Murray, *J. Appl. Phys.* **35**, 2349 (1964).
7. L. M. Frantz and J. S. Nodvik, *ibid.* **34**, 2346 (1963).
8. D. A. Stetser and A. J. DeMaria, *Appl. Phys. Letters* **9**, 118 (1966).
9. M. DiDomenico, Jr., *J. Appl. Phys.* **35**, 2870 (1964); A. Yariv, *ibid.* **36**, 388 (1965).
10. L. E. Hargrove, R. L. Fork, M. A. Pollack, *Appl. Phys. Letters* **5**, 4 (1964).
11. M. H. Crowell; *IEEE (Inst. Elec. Electron. Engrs.) J. Quantum Electron.* **1**, 12 (1965).
12. A. J. DeMaria, C. M. Ferrar, G. E. Danielson, Jr., *ibid.*, p. 22.
13. A. J. DeMaria, D. A. Stetser, H. A. Heynau, *ibid.*, p. 174 (paper presented at the Intern. Conf. on Quantum Electronics, 1966).
14. T. Deutsch, *ibid.* **7**, 80 (1965).
15. M. DiDomenico, Jr., J. E. Geusic, H. M. Marcos, R. G. Smith, *ibid.* **8**, 180 (1966).
16. D. A. Stetser and A. J. DeMaria, *ibid.* **9**, 118 (1966).
17. S. E. Harris and R. Targ, *ibid.* **5**, 202 (1964).
18. A. J. DeMaria, *J. Appl. Phys.* **34**, 2984 (1963).
19. L. C. Foster, M. D. Ewy, C. B. Crumly, *Appl. Phys. Letters* **6**, 6 (1965).
20. G. A. Massey, M. K. Oshman, R. Targ, *ibid.*, p. 10.
21. A. J. DeMaria and D. A. Stetser, *ibid.* **7**, 71 (1965).
22. H. W. Mocker and R. J. Collins, *ibid.*, p. 270.
23. C. C. Cutler, *Proc. I.R.E. (Inst. Radio Engrs.)* **43**, 140 (1955).
24. R. L. Kohn and R. H. Pantell, *Appl. Phys. Letters* **8**, 231 (1966).
25. W. R. Sooy, *ibid.* **7**, 36 (1965).
26. B. H. Soffer, *J. Appl. Phys.* **35**, 2551 (1964); F. J. McClung and D. Weiner, *IEEE (Inst. Elec. Electron. Engrs.) J. Quantum Electron.* **1**, 94 (1965).
27. M. Hercher, *Appl. Phys. Letters* **7**, 39 (1965).
28. N. Bloembergen, P. Lallemand, A. Pine, *IEEE (Inst. Elec. Electron. Engrs.) J. Quantum Electron.* **2**, 246 (1966); N. Bloembergen and P. Lallemand, *Phys. Rev. Letters* **16**, 81 (1966); P. Lallemand, *Appl. Phys. Letters* **8**, 276 (1966).
- 28a. *Note added in proof:* After this article was written, this experiment was performed by J. A. Armstrong [*Appl. Phys. Letters* **10**, 16 (1967)] and W. H. Glenn, Jr., and M. J. Brienza, *ibid.* (15 Apr. 1967). Armstrong reported pulse widths of 4×10^{-12} second. Glenn and Brienza reported pulse widths of 8×10^{-12} second, but they found that the time duration of the pulses changed from pulse to pulse within the pulse train up to a maximum pulse width of 25×10^{-12} second. The reason for the order-of-magnitude discrepancy between the results of the experi-
- ments performed by Armstrong and by Glenn and Brienza and the spectrum density measurements reported earlier in this article (see Figs. 11, 13, and 15) is not known.
29. A. A. Vuylsteke, *J. Appl. Phys.* **34**, 1615 (1963).
30. W. R. Hook, R. H. Dishington, R. P. Hilberg, *Appl. Phys. Letters* **9**, 125 (1966).
31. R. V. Ambartsumyan, N. G. Basov, V. S. Zuev, P. G. Kryukov, V. S. Letokhov, *JETP Letters (English Transl.)* **4**, 12 (1966).
32. A. W. Penney, Jr., and H. A. Heynau, *Appl. Phys. Letters* **9**, 257 (1966).
33. M. Michon, J. Ernest, R. Auffret, *Phys. Letters* **21**, 514 (1966).
34. A. J. DeMaria, R. Gagosz, H. A. Heynau, A. W. Penney, Jr., G. Wisner, *Appl. Phys. Letters*, in press.
35. A. G. Fox and T. Li, *Bell System Tech. J.* **40**, 453 (1961).
36. H. A. Heynau, *Proc. IEEE (Inst. Elec. Electron. Engrs.)* **53**, 2145 (1965).
37. R. N. Lewis, E. A. Jung, G. L. Chapman, L. S. VanLoon, F. A. Romanowski, *IEEE (Inst. Elec. Electron. Engrs.) Trans. Nuclear Sci.* **13**, 84 (1966).
38. The work discussed in this article was supported in part by the U.S. Army Missile Command and the U.S. Air Force Systems Command.

Collaboration for Accelerating Progress in Medical Research

Albert B. Sabin

Fully recognizing the importance of assuring that the laboriously acquired existing knowledge not remain on library shelves to be admired like great works of art in museums but be expeditiously put to work for human welfare, I nevertheless wish to limit my present statement to the problems involved in the acquisition of the new knowledge that is needed for the elimination or alleviation of human disease and for the improvement of human health.

Let me first of all agree with those who stress the importance of the individual scientist's search for knowledge for its own sake as the very foundation of scientific endeavor that must continue to be supported and ex-

panded if science is to provide the means for the solution of the many problems of importance to human welfare. Unlike many other types of scientific research, medical research is by its very nature oriented toward specific goals directly related to human health. As I see it, the real issue in medical research is not so much the maintaining of a proper balance between so-called basic research, designed chiefly to provide understanding of life processes, and so-called applied or mission-oriented research, designed to achieve a well-defined objective like the prevention, alleviation, or cure of a disease—because to achieve the latter you must invariably also engage in the former—as it is the proper definition of important specific targets that call for and are ready for a concentrated, well-planned, and coordinated research effort. As more and more people enter the field of medical research and more

and more money becomes available for it, there is unfortunately an increasing proportion of persons who choose to work on little problems that they can handle by themselves or in collaboration with small groups of junior investigators. The important issue, it seems to me, is whether enough is being done to develop *acceptable* mechanisms for coordinated and cooperative research—regardless of whether it be for achieving the initial basic understanding or the ultimate control of a disease—to attack those larger and more complex problems whose solution can be markedly retarded if the necessary work is left to the chance interests and uncoordinated efforts of the individual scientists. My own conclusion is that much more needs to be done than is now being done, and in what follows I examine the question of whose responsibility it is to plan for a more concentrated attack on the more complex disease problems, and to consider new mechanisms for planning, for establishing priorities for funding—because money for research, like money for everything else, must be budgeted—and for implementing the decisions that are reached. The decisions that I have in mind would have to be made by the most competent scientists, who will have to do the work; by the administrators, in conjunction with their advisory councils, who will have to establish priorities on the basis of relative importance and need; and by the Congress representing the public, from whom the money will have to come for translating reasonable plans into working projects.

The author is Distinguished Service Professor of Research Pediatrics, University of Cincinnati College of Medicine, Cincinnati, Ohio. This article is adapted from testimony presented on 16 March before the Senate Subcommittee on Government Research.